CHAPTER 169

BUOYANCY-DRIVEN GRAVITATIONAL SPREADING

by

Robert C. Y. Koh[1]

Introduction

It frequently occurs in environmental fluid mechanics that a mass of leas heavy fluid spreads horizontally on top of a heavier one or a more homogeneous parcel of fluid spreads within a stratified one. Examples of auch phenomena include spreading of diluted sewage effluent either at the surface or in a submerged layer, the spreading of heated effluent discharged from power plants, and the spreading of oil on the surface of the sea. The general problem is rather complex, being influenced not only by the buoyancy but also by momentum, ambient turbulence and flow, surface tenaion, waves, wind and other complicating factora. This paper attempts to examine gravitational buoyancy-driven flow in a homogeneous otherwise motionless ambient by casting it in the form of an initial value problem. Several assumptions are made and two empirical coefficients are introduced which must be determined from experiments. Experimental data are also preaented, compared with the results of the analysis and the empirical coefficients determined. Previous investigations on aimilar problems include Sharp (1969, 1971), Koh and Fan (1968, 1969, 1971), and Koh and Chang (1973).

Formulation of the Problem

The fluid dynamic problem which will be considered in this paper is the time dependent spreading of one fluid on top of a heavier fluid. Both the two-dimenaional and the axisymmetric cases will be examined. In each geometrical configuration, both the instantaneous and the continuous discharge cases will be inveatigated. The derivation will be detailed only for the two-dimensional case. Results for the axisymmetric case will be presented without detailed derivations.

Consider that at time $t = 0$, a mass of buoyant fluid of volume A, linear dimensions characterized by a and b and density $\rho_o - \Delta\rho$ is released from a state of rest on the aurface of a deep reservoir containing fluid of density ρ_o (see Fig. 1). It will be aasumed that there is little mixing between the two fluids and that the shape of the buoyant fluid remains similar from one instant to another while it spreads. One expects that b will increaae with time and a will decrease with time. For the moment, it will be convenient to assume that the motions in the heavier fluid is insignificant.

Figure 2 shows half of the buoyant fluid mass which will be considered as a free body. Assuming for the moment that the pressure distribution is hydrostatic, the buoyancy ia seen to induce a net horizontal force of

$$\frac{1}{2} g' a^2 = \frac{1}{2} g \frac{(\rho_o - \rho) a^2}{\rho}$$

In actuality, the pressure distribution is not hydrostatic. The departure of the presaure distribution from being hydroatatic will be accounted for by a horizontal force term which resembles that for hydrodynamic form drag and will be written

$$-\frac{C_D}{2} \rho a \left(\frac{db}{dt}\right)^2$$

the negative sign to indicate that the force is in opposition to the motion. There is another horizontal force tending to retard the spreading fluid, namely,

[1]Research Associate in Environmental Engineering Science, California Institute of Technology.

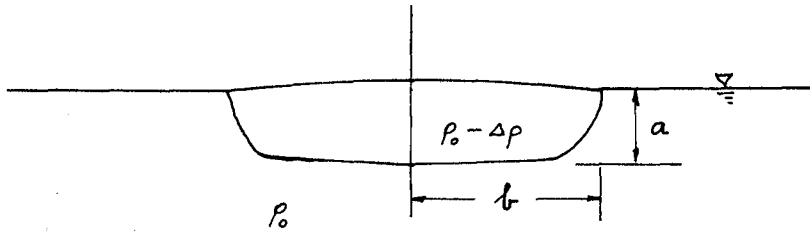

Figure 1. Definition Sketch.

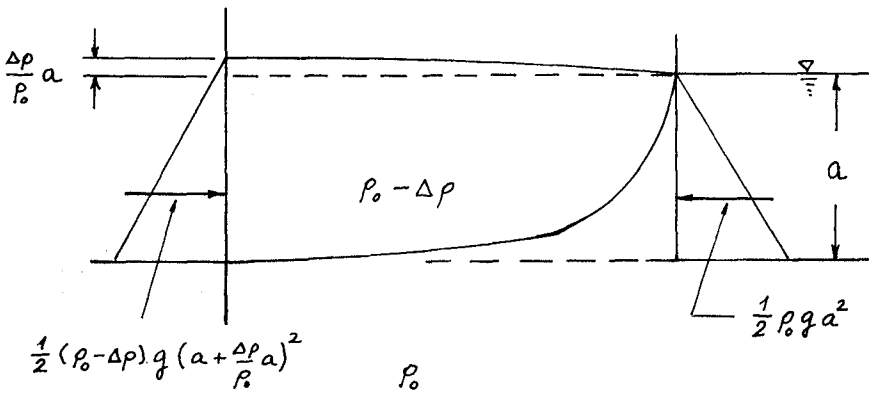

Figure 2. Pressure Forces on Half a Spreading Element.

that on the interface between the two fluids similar to a skin friction. It will be assumed that this force is

$$-\nu C_F \frac{b}{a}\frac{db}{dt}$$

The net imbalance of these forces must be equal to the net rate of change of momentum of the free body. Thus the equation of motion is

$$\frac{d}{dt}\left[(C_a ab)\frac{d}{dt}(C_g b)\right] = \frac{1}{2} g' a^2 - C_D \frac{g}{2}\left(\frac{db}{dt}\right)^2 - C_F \nu \frac{b}{a}\frac{db}{dt} \qquad (1)$$

where $C_a ab$ is the cross-sectional area of the free body and $C_g b$ is the distance from the origin to the center of mass of the cross-section. These quantities C_a, C_g are coefficients which depend only on the geometrical shape of the cross-section . By the assumption of similarity in shape, they will be constants. Table 1 gives values for C_g and C_a for several shapes.

Table 1

Shape	Geometry	C_g	C_a
rectangle		1/2	1
ellipse		$4/3\pi$	$\pi/4$
truncated trapezoid		4/9	3/4

For the case of no mixing between the two fluids, the equation for conservation of mass is simply

$$C_a ab = A = \text{constant} \qquad (2)$$

for the case of instantaneous release. For a continuous discharge, it is

$$C_a ab = qt \qquad (3)$$

where q is the discharge rate which accounts for half of the spreading layer. It should be noted that mixing can be allowed in this formulation by properly modifying the equations. Also, an apparent mass coefficient could have been introduced on the left-hand side of the equation. Neither will be done herein for simplicity. The derivation including these effects can be found in Koh and Chang (1973).

For definiteness, the shape of the spreading layer will be taken to be elliptical so that the coefficients C_a, and C_g are $\pi/4$ and $4/3\pi$ respectively. Equation 1 then becomes, after using either (2) or (3),

$$\frac{d^2 b}{dt^2} = \frac{6}{\pi}\frac{g' A}{b^2} - \frac{3}{2}\frac{C_D}{b}\left(\frac{db}{dt}\right)^2 - \frac{3\pi^2}{16}\frac{C_F \nu}{A^2} b^2 \frac{db}{dt} \qquad (4)$$

and

$$\frac{d}{dt}\left(t\frac{db}{dt}\right) = \frac{6}{\pi} g' q \frac{t^2}{b^2} - \frac{3}{2} C_D \frac{t}{b}\left(\frac{db}{dt}\right)^2 - \frac{3\pi^2}{16}\frac{C_F \nu}{q^2}\frac{b^2}{t}\frac{db}{dt} \qquad (5)$$

for the instantaneous release and continuous discharge respectively.

In the axisymmetric case, defining the shape of the spreading fluid to be half an ellipsoid of revolution, the equations analogous to (1), (2) and (3) are readily deduced to be

$$\frac{d}{dt}\left\{\frac{\pi ab^2}{16}\frac{db}{dt}\right\} = \frac{g' a^2 b}{3} - C_D \frac{ab}{4}\left(\frac{db}{dt}\right)^2 - C_F \nu \frac{b^2}{a}\frac{db}{dt} \qquad (1a)$$

$$\frac{2\pi}{3} ab^2 = V \tag{2a}$$

$$\frac{2\pi}{3} ab^2 = Q_o t \tag{3a}$$

From theae equations, one can derive the equations analogous to (4) and (5) to be

$$\frac{d^2b}{dt^2} = \frac{8g'V}{\pi^2}\frac{1}{b^3} - \frac{8C_D}{\pi}\frac{1}{b}\left(\frac{db}{dt}\right)^2 - \frac{64\pi}{9V^2} C_F \nu b^4 \frac{db}{dt} \tag{4a}$$

and

$$\frac{d}{dt}\left[t\frac{db}{dt}\right] = \frac{8g'Q}{\pi^2}\frac{t}{b^3} - \frac{8C_D}{\pi}\frac{t}{b}\left(\frac{db}{dt}\right)^2 - \frac{64\pi}{9Q^2} C_F \nu \frac{b^4}{t}\frac{db}{dt} \tag{5a}$$

Equations (4),(5),(4a) and (5a) will form the basis of the investigation in the remainder of this paper.

Normalization

The equations (4),(5),(4a), and (5a) will be normalized by choosing characteristic length b_o and characteristic time t_o so as to make the resulting dimensionless equations as simple as possible. This leads to the choices for b_o and t_o as tabulated in Table 2. The dimensionless equations which result become

Table 2

	Two-dim. instantaneous	Two-dim. continuous	Axisymmetric instantaneous	Axisymmetric continuous
t_o	$\left(\frac{16A^2}{3\pi^2\nu}\right)^{3/7}\left(\frac{\pi}{6g'A}\right)^{2/7}$	$\left(\frac{16q^2}{3\pi^2\nu}\right)\left(\frac{\pi}{6g'q}\right)^{2/3}$	$\frac{512\nu g'}{9\pi V}$	$\left(\frac{\pi^2}{8g'Q}\right)^{1/2}\left(\frac{9Q^2}{64\pi\nu}\right)^{1/2}$
b_o	$\left(\frac{16A^2}{3\pi^2\nu}\right)^{2/7}\left(\frac{6g'A}{\pi}\right)^{1/7}$	$\left(\frac{16g^2}{3\pi^2\nu}\right)\left(\frac{\pi}{6g'q}\right)^{1/3}$	$\left(\frac{\pi^2}{8g'V}\right)^{1/4}$	$\left(\frac{\pi^2}{8g'Q}\right)^{1/8}\left(\frac{9Q^2}{64\pi\nu}\right)^{3/8}$

$$\frac{d^2\zeta}{dt^2} = \frac{1}{\zeta^2} - \frac{3}{2} C_D \frac{1}{\zeta}\left(\frac{d\zeta}{dt}\right)^2 - C_F\zeta^2\frac{d\zeta}{dt} \tag{6}$$

$$\frac{d}{dt}\left(t\frac{d\zeta}{dt}\right) = \frac{t^2}{\zeta^2} - \frac{3}{2} C_D \frac{t}{\zeta}\left(\frac{d\zeta}{dt}\right)^2 - C_F\frac{\zeta^2}{t}\frac{d\zeta}{dt} \tag{7}$$

$$\frac{d^2\zeta}{dt^2} = \frac{1}{\zeta^3} - \frac{8C_D}{\pi}\frac{1}{\zeta}\left(\frac{d\zeta}{dt}\right)^2 - C_F\zeta^4\frac{d\zeta}{dt} \tag{6a}$$

$$\frac{d}{dt}\left(t\frac{d\zeta}{dt}\right) = \frac{t^2}{\zeta^3} - \frac{8C_D}{\pi}\frac{t}{\zeta}\left(\frac{d\zeta}{dt}\right)^2 - C_F\frac{\zeta^4}{t}\frac{d\zeta}{dt} \tag{7a}$$

where $\zeta = b/b_o$, $t = t/t_o$, corresponding to (4), (5), (4a), and (5a) respectively. Once the solution $\zeta(t)$ is obtained, the thickness a (or dimensionless $\eta = a/a_o$,

with appropriately chosen a_o) can be obtained from the continuity equation (2), (3),(2a), and (3a).

Each of the equations (6),(7),(6a), and (7a) will give solutions in the form $\zeta(t;C_F,C_D,\zeta_o,\zeta_o')$ where the four quantities C_F,C_D,ζ_o,ζ_o' are parameters needed to specify the solution. Here ζ_o and ζ_o' are the values of ζ and $d\zeta/dt$ at $t=0$. It is possible to have included C_F in the normalizing factors b_o and t_o. This is not done to allow the effect of C_F to show up more clearly and also allow comparison with experiments to be more meaningful.

Approximate Solution for Small Time

From physical reasoning, it can be expected that for small time, the term involving C_F would be unimportant since ζ would be small. Moreover, for the instantaneous release cases (eqs. 6 and 6a), the term involving C_D would also be insignificant for small t since $d\zeta/dt$ would be small. Thus, for small t, the equations 6 and 6a can be written

$$\frac{d^2\zeta}{dt^2} = \frac{1}{\zeta^2}$$

and

$$\frac{d^2\zeta}{dt^2} = \frac{1}{\zeta^3}$$

subject to the initial conditions $\zeta(0)=\zeta_o,\zeta'(0)=0$. The solutions can be obtained by quadratures. For example, for the continuous release case,

$$\zeta = \zeta_o\sqrt{1+t^2/\zeta_o^4}$$

This represents the transient start-up period. The solution for the instantaneous case is more complex and will not be displayed.

Approximate Solution for Intermediate Time

For times not too large, physical considerations again lead to the approximation of ignoring the term involving C_F in the equations (6),(7),(6a) and (7a). It is now fruitful to examine solutions of the form $\zeta = Bt^\alpha$. Substituting this into each of the equations (ignoring the C_F terms) results in the following values for α, and the resulting time dependence for ζ (width) and η (thickness).

	2-dim. inst.	2-dim. cont.	axisym. inst.	axisym. cont.
α	2/3	1	1/2	3/4
$\zeta \propto$	$t^{2/3}$	t	$t^{1/2}$	$t^{3/4}$
$\eta \propto$	$t^{-2/3}$	1	t^{-1}	$t^{-1/2}$

These represent the circumstance when inertia balances the buoyancy driving force.

Approximate Solution for Large Time

For large time, ζ becomes very large, thus making the term involving C_F dominant. Physically this means that the interfacial shear is the dominant resistive force. If one now balances the driving force by this term (i.e., ignore the left-hand side as well as the C_D term in equations (6),(7),(6a), and (7a)), and seek solutions of the form $\zeta = B_1 t^{\alpha_1}$, one finds

	2-dim. inst.	2-dim. cont.	axisym. inst.	axisym. cont.
α_1 =	1/5	4/5	1/8	1/2
ζ $\propto$	$t^{1/5}$	$t^{4/5}$	$t^{1/8}$	$t^{1/2}$
η $\propto$	$t^{-1/5}$	$t^{1/5}$	$t^{-1/4}$	1

These represent the circumstance when interfacial shear balances the buoyancy driving force. It is worth noting that the behavior of η (thickness) as function of t (time) is fundamentally different between the two-dimensional and axisymmetric cases for continuous discharge. Whereas $\eta \sim t^{1/5}$ in the two-dimensional case, η tends to a constant value in the axisymmetric case. Physically, this means that the thickness will continue to grow ad infinitum in the former while it would not in the latter case.

Overall Solutions

From the above discussion it is seen that after a brief start-up period, the solution for the extent of the spreading layer can be represented in each case by a power law in time where the power changes from one value to a second value as time progresses. It should be noted that the above results could have been obtained from simple dimensional arguments. The purpose for extracting them herein is to provide more insight into the relationships among the various phenomena represented by the various terms in the equations.

In general, the equations (6),(7),(6a),(7a) including all the terms can only be solved numerically. This has been done using a fourth order Range Kutta algorithm. The results for example cases for equation (6) is shown in Figure 3.

Comparison with Experiments

The results of the analysis will now be compared with laboratory experiments. The writer wishes to acknowledge Messrs. C. Almquist, P. J. W. Roberts and J. C. Chen who actually performed these experiments. While these individuals have performed a larger number of experiments, only example runs are presented herein for comparison purposes. The experimental data used for comparison in the following are shown tabulated in Table 3.

Two-Dimensional Instantaneous Release

These experiments were performed by C. Almquist (1973) as a term project for a course in the Environmental Engineering option at California Institute of Technology. The laboratory tank used was 5 inches wide by 18 inches deep by 16 feet long. It is filled with salt water (sp. gr. $\approx$ 1.020). A trough at the surface at one end of the tank containing less dense dyed water in hydrostatic equilibrium with the water in the tank is released at $t = 0$ by removal of a partition (see Figure 4a). The subsequent motion of the spreading layer is then timed. The density difference and the amount of the released fluid was varied over a factor of 4 and 9 respectively resulting in a total of twenty experiments. Figure 5 shows the data for four example runs together with the predictions from equation (4). In obtaining this comparison, the initial conditions were chosen to be the values of b and db/dt (dimensional values) at the beginning of the data. The values of C_D and C_F are chosen to obtain a good fit between the prediction and the experiment. However, the same value for C_D and the same value of C_F were used in all four comparisons. This comparison indicates that the predictions are quite good. Moreover, the values for C_D and C_F (0.85 and 0.4 respectively) are what might be expected being of order unity.

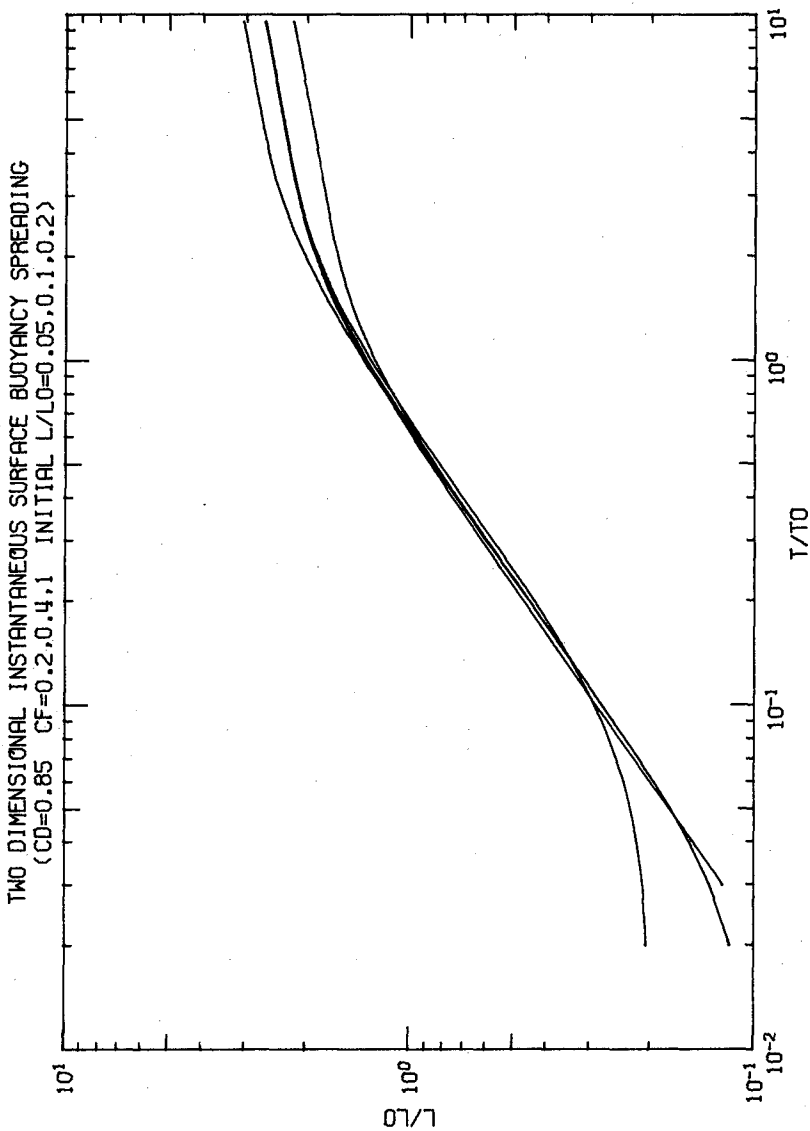
TWO DIMENSIONAL INSTANTANEOUS SURFACE BUOYANCY SPREADING
(CD=0.85 CF=0.2,0.4,1 INITIAL L/LO=0.05,0.1,0.2)
L/LO
T/TO
10¹
10⁰
10⁻¹
10⁻²
10⁻¹
10⁰
10¹

Figure 3.

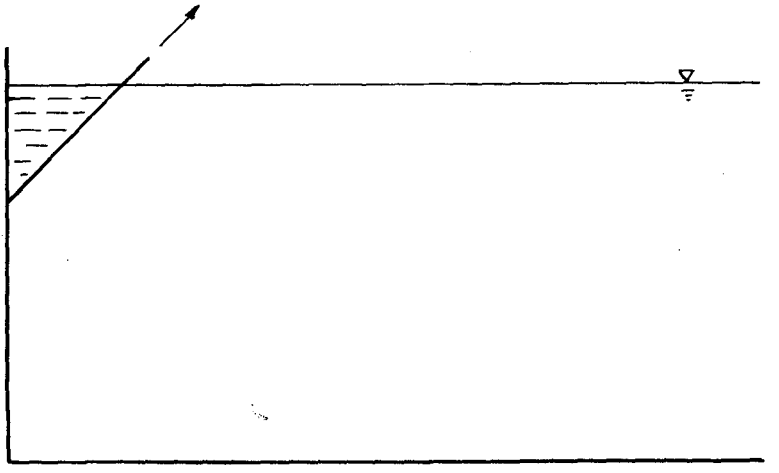

(a) instantaneous release

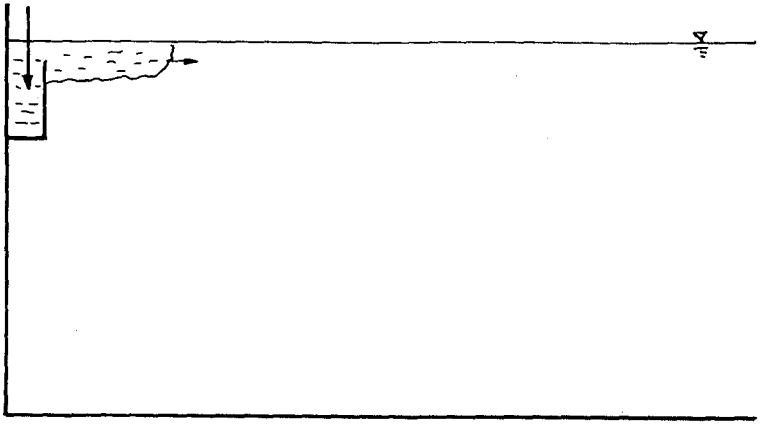

(b) continuous release

Figure 4. Schematic of Laboratory Set-Up for Two-Dimensional Surface Release Experiments.

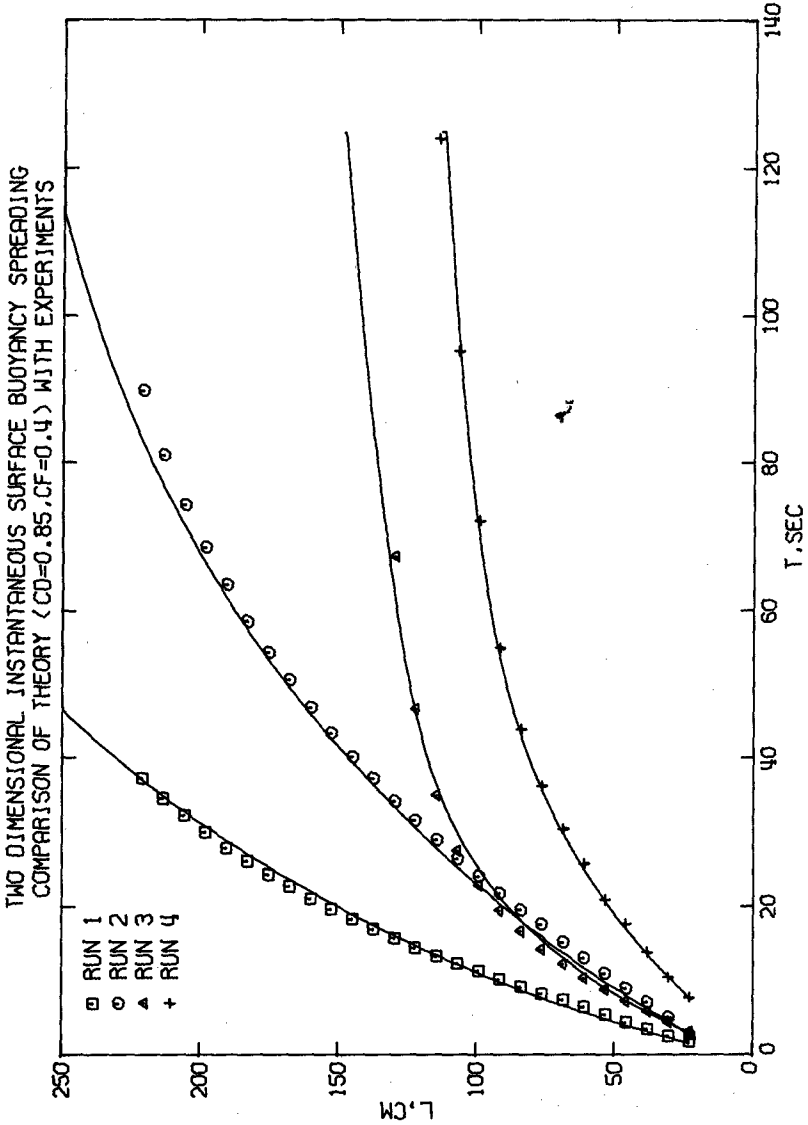
TWO DIMENSIONAL INSTANTANEOUS SURFACE BUOYANCY SPREADING
COMPARISON OF THEORY (CD=0.85,CF=0.4) WITH EXPERIMENTS
RUN 1
RUN 2
RUN 3
RUN 4
L,CM
T,SEC
0
50
100
150
200
250
0
20
40
60
80
100
120
140

Figure 5.

Table 3

Basic Experimental Parameters

(a) Two-Dimensional Instantaneous Release

Run No.	A (cm^2)	$\Delta\rho/\rho$
1	116.	0.016
2	116.	0.004
3	29.	0.016
4	29.	0.004

(b) Two-Dimensional Continuous Release

Run No.	q (cm^2/sec)	$\Delta\rho/\rho$
1	2.09	0.0036
2	4.33	0.0038
3	4.06	0.0066
4	3.92	0.0145

(c) Two-Dimensional Submerged Continuous Release

Run No.	q cm^2/sec	$\Delta\rho/\rho$	Depth cm
1	0.108	0.0240	16.3
2	0.189	0.0252	16.1
3	0.344	0.0244	8.1

(d) Axisymmetric Submerged Continuous Release

Run No.	Q cc/sec	$\Delta\rho/\rho$	Depth cm
1	41.6	0.051	11.7
2	37.5	0.013	23.4
3	13.5	0.066	5.9
4	13.5	0.022	5.9
5	13.5	0.017	5.9

The same data are shown plotted in Figure 6 in non-dimensional form. The curve shown is for $C_D = 0.85$ and $C_F = 0.4$ obtained as the solution to equation (6) (in dimensionless variables). The initial start-up period is ignored in this solution hence the lack of fit for small t. It should also be pointed out that the initial conditions used in the predictive solution, as a consequence, is independent of the data. From this comparison, it is seen that the analyses does, in fact, conform to the data quite well.

Two-Dimensional Continuous Surface Release

These experiments were also performed by C. Almquist under the same circumstances in the same tank. The only difference in the procedure is in the mode of introduction of the buoyant fluid. In this case, the buoyant fluid is allowed to be discharged continuously at the surface at one end of the tank from a structure as shown in Figure 4b. The supply of the buoyant fluid is via a constant head tank. Comparison of the results of four of the experiments are shown in Figure 7 where the curve is obtained by solving equation (7) using $C_D = 0.5$, and $C_F = 5$.

Two-Dimensional Continuous Submerged Release

These experiments were performed by P. J. W. Roberts in a much larger tank than the previous experiments. The buoyant fluid is now introduced at the bottom of the tank, allowed to rise to the surface and then spread horizontally on the surface. A schematic of the experimental setup is shown in Figure 8. It should be pointed out that while equation (7) is still applicable to this case, interpretation of the coefficients C_D and C_F must be viewed somewhat differently. Whereas in the surface release case, the water depth in the tank is much larger than the thickness of the spreading layer, this is no longer true in the submerged case. More importantly, in this case, mixing occurs during the rise of the buoyant water from the discharge point at the bottom to the surface. An entrainment undercurrent is set up whose direction is opposite to that of the spreading layer. One must, therefore, expect both C_D and C_F to be larger than in the previous experiments. In the case when the entrainment is significant, one expects C_D to be larger by a factor of approximately 3 for the case when the spreading layer is approximately 1/3 of the total depth as was observed to be the case. Comparison of these experiments with the solution to eq. (7) with $C_D = 2.5$ and $C_F = 14.5$ is shown in Figure 9 where again the data appears to confirm the analysis.

Axisymmetric Continuous Submerged Release

These experiments were performed by J. C. Chen in the same laboratory basin as the two-dimensional submerged release experiments. A 6 mm diameter round orifice is placed at the bottom of the basin. Injection is started and overhead photographs taken at discrete times to record the spread of the dyed buoyant fluid. The normalized variables ζ and t for five of these experiments are shown in Figure 10 together with the analytical results ($C_D = 0.2$, $C_F = 0.05$). The comparison is seen to be reasonable.

It should be noted here that in the submerged release cases, the buoyant discharge undergoes a certain amount of dilution before reaching the surface and spreading. Thus the value of the discharge rate is actually larger than the discharge from the orifice by a factor equal to the average dilution. The buoyancy flux, of course, is still unchanged. In plotting the experimental points in Figures 9 and 10, the discharge rates have been calculated on the basis of simple plume theory with S_a given by

$$S_a = 0.38 \frac{y(g_o' q_o)^{1/3}}{q_o}$$

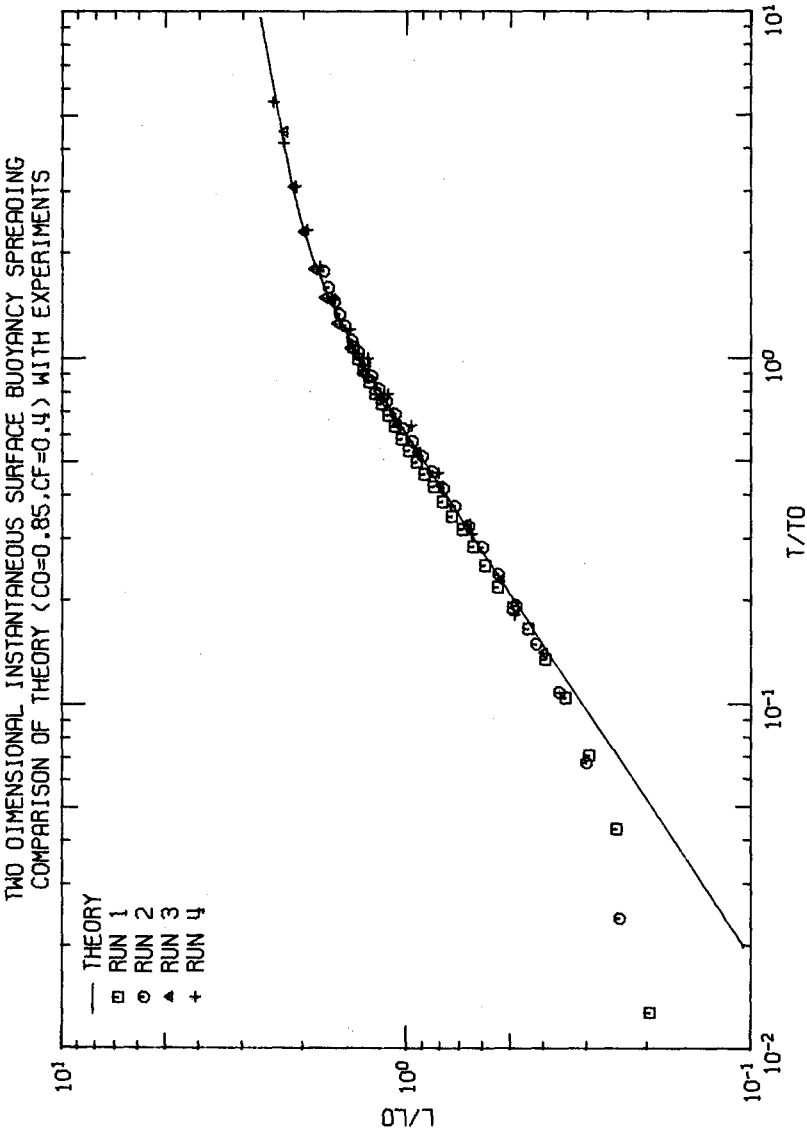
TWO DIMENSIONAL INSTANTANEOUS SURFACE BUOYANCY SPREADING
COMPARISON OF THEORY (CO=0.85,CF=0.4) WITH EXPERIMENTS
THEORY
RUN 1
RUN 2
RUN 3
RUN 4
L/LO
T/TO
10^{1}
10^{0}
10^{-1}
10^{-2}

Figure 6.

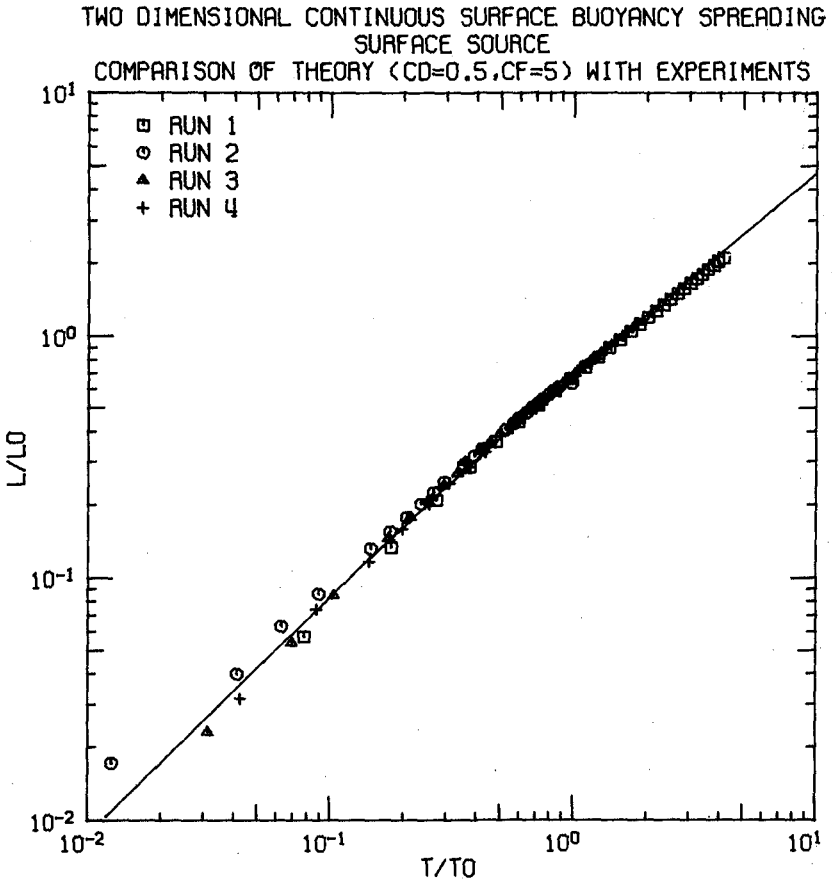
TWO DIMENSIONAL CONTINUOUS SURFACE BUOYANCY SPREADING
SURFACE SOURCE
COMPARISON OF THEORY (CD=0.5,CF=5) WITH EXPERIMENTS
RUN 1
RUN 2
RUN 3
RUN 4
L/LO
T/TO
10^{1}
10^{0}
10^{-1}
10^{-2}

Figure 7.

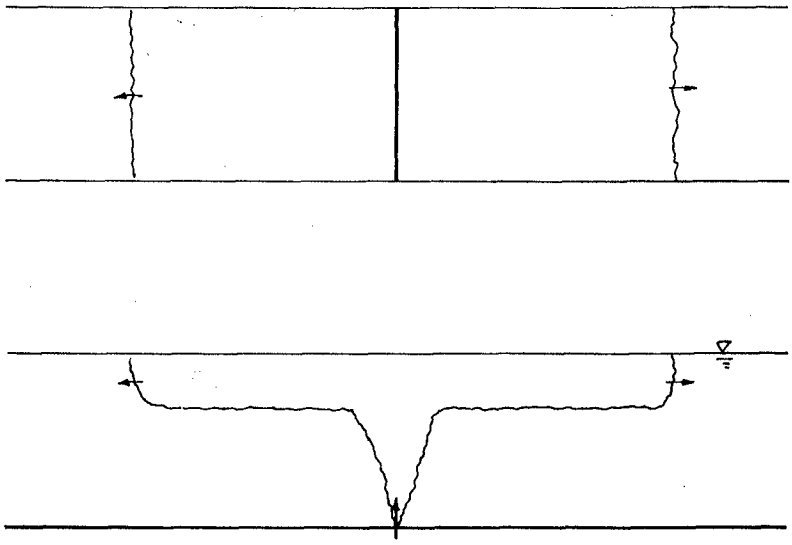

Figure 8. Schematic of Laboratory Set-Up for Two-Dimensional Continuous Submerged Release Experiments.

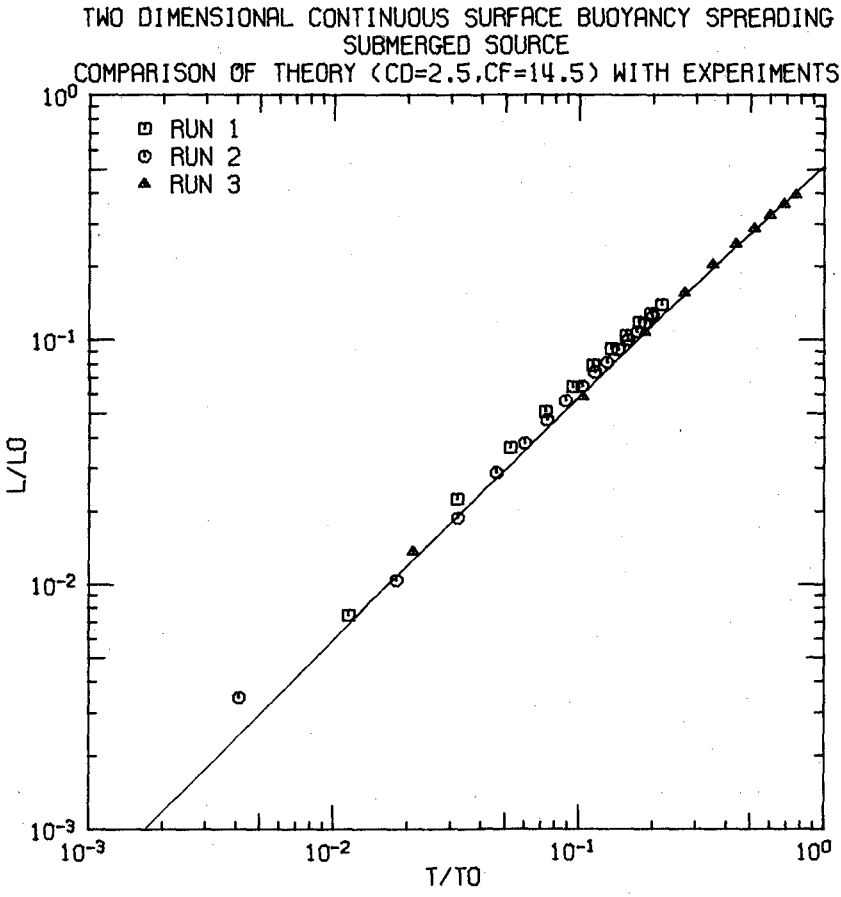
TWO DIMENSIONAL CONTINUOUS SURFACE BUOYANCY SPREADING
SUBMERGED SOURCE
COMPARISON OF THEORY (CD=2.5,CF=14.5) WITH EXPERIMENTS
RUN 1
RUN 2
RUN 3
L/LO
T/TO
10^{0}
10^{-1}
10^{-2}
10^{-3}

Figure 9.

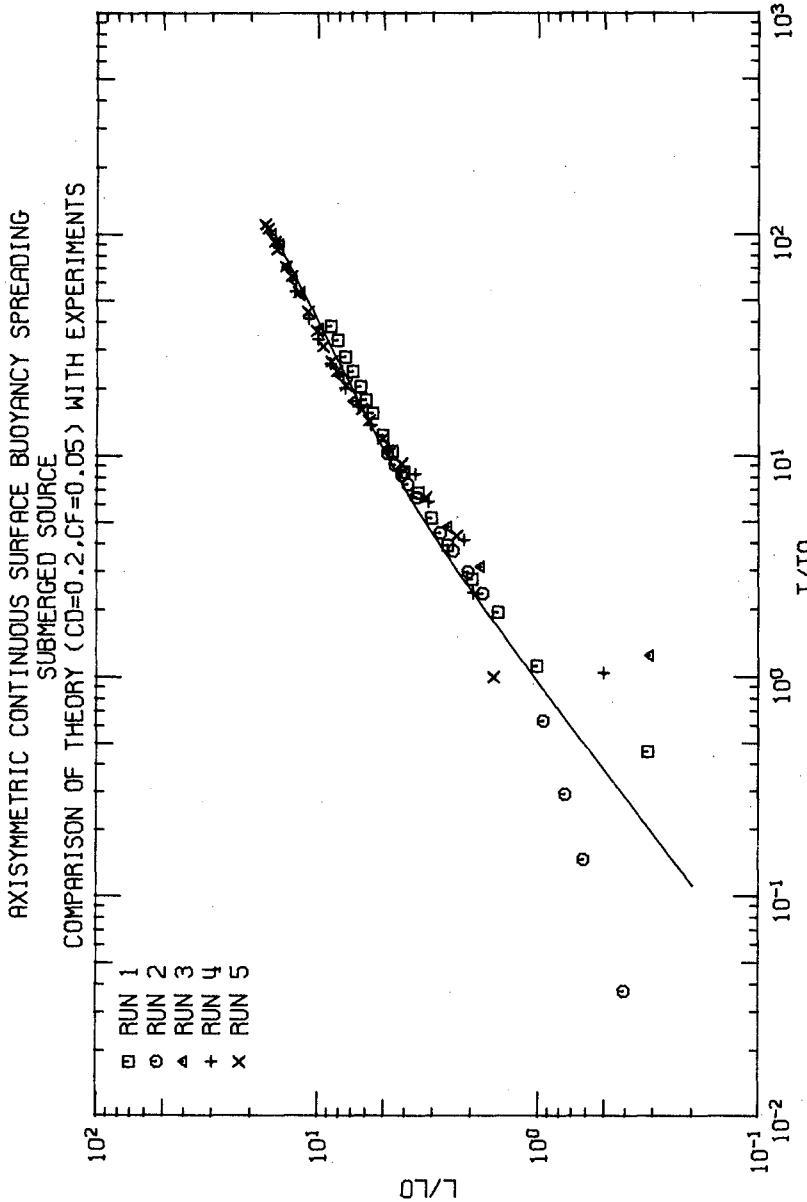
AXISYMMETRIC CONTINUOUS SURFACE BUOYANCY SPREADING
SUBMERGED SOURCE
COMPARISON OF THEORY (CD=0.2,CF=0.05) WITH EXPERIMENTS
RUN 1
RUN 2
RUN 3
RUN 4
RUN 5
L/LO
T/TO
10^{2}
10^{1}
10^{0}
10^{-1}
10^{-2}
10^{-1}
10^{0}
10^{1}
10^{2}
10^{3}

Figure 10.

$$S_a = 0.16 \frac{y^{5/3}(g'_o Q_o)^{1/3}}{Q_o}$$

(S_a = average dilution).

Practical Applications

It appears at first glance that the results obtained in the previous sections are of little practical value since in practice, neither two-dimensionality nor axial-symmetry obtains. It will be shown in this section how the results can be utilized to deduce some properties of the flow field which are of great practical value.

(a) Thickness of surface sewage field.

Major coastal discharges of sewage effluent into the ocean frequently employ long diffusion structures (on the order of several thousand feet long) at a depth of approximately 200 ft. Many small ports along the diffuser discharges the effluent in such a way as to approximate a long line source of effluent. It has been found experimentally that, in the event where the ocean is uniform in density and motionless, simple line plume theory gives good predictions of dilution factors (see e.g., Koh and Brooks, 1975). The centerline dilution, S_c according to that theory is simply

$$S_c = 0.38 \frac{(g'_o q_o)^{1/3} y}{q_o} \tag{8}$$

The average dilution S_a is $\sqrt{2}\, S_c$. Here $(g'_o q_o)$, q_o, and y are the buoyancy flux and discharge per unit length, and vertical distance from the diffuser ($g'_o = g(\rho_o - \rho)/\rho$; g = gravitational acceleration, ρ = density of effluent, ρ_o = density of sea water). Referring to Figure 11, there is seen to be an uncertainty in application of equation (8) in that one does not know what value of y to use. Whereas buoyant plume theory is developed for an infinite fluid, the presence of the ocean surface deflects the sewage field to spread on the surface. The value of y to be substituted into equation (8) to obtain the surface dilution should logically be (d-a) where d is the depth and a the thickness of the sewage field (see Figure 11). The thickness of the surface field a will now be estimated from the results of analyses in this paper. It should first be noted that the thickness a(t) defined in the two-dimensional continuous release case analyzed previously is the quantity of interest. As a function of time, it starts at zero, grows to a constant value, remains constant until interfacial shear forces become important, whereupon it grows as $t^{1/5}$ without limit. For practical problems, the $t^{1/5}$ growth is of little significance since by the time this would occur, the two-dimensionality assumption breaks down. (It may be noted that in the three-dimensional continuous release case, the thickness tends to a constant.) Given that shear is unimportant, one may write equation (5) as

$$\frac{d}{dt}\left(t \frac{db}{dt}\right) = \frac{6}{\pi}(g'q) \frac{t^2}{b^2} - \frac{3}{2} C_D \frac{t}{b}\left(\frac{db}{dt}\right)^2 \tag{9}$$

with solution

$$b = \gamma t \tag{10}$$

where

$$\gamma = \left[\frac{\frac{6}{\pi} g'q}{1 + \frac{3}{2} C_D}\right]^{1/3}$$

but

$$qt = \frac{\pi}{4} ab \tag{11}$$

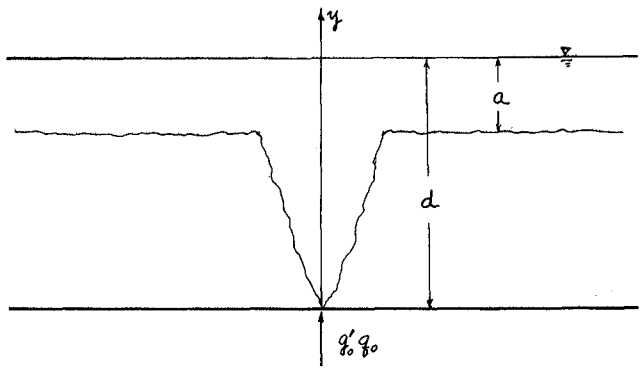

Figure 11. Definition Sketch.

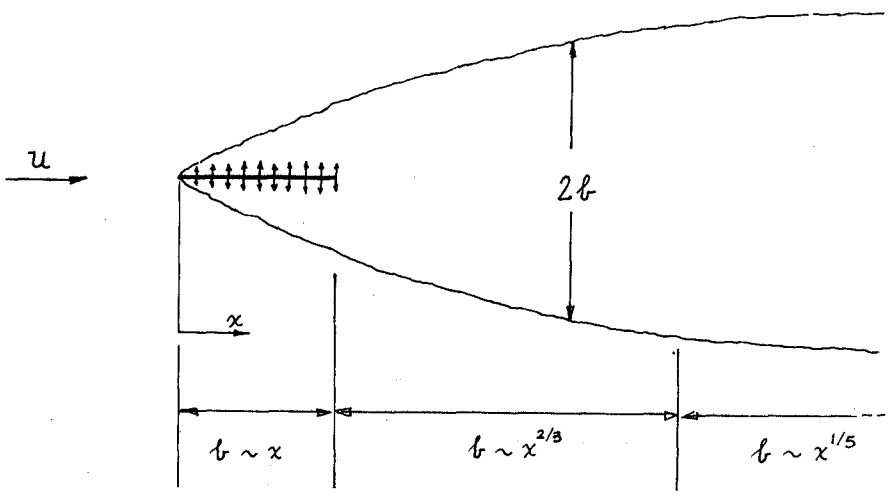

Figure 12. Schematic Plan View of Wastewater Plume.

so that

$$a = \frac{4q}{\pi\gamma} = \frac{4q}{\pi}\left[\frac{1+\frac{3}{2}C_D}{\frac{6}{\pi}g'q}\right]^{1/3} \qquad (12)$$

It may be seen that, in the present case, $g'q = g'_o q_o/2$, and $q = S_a q_o/2$ where the factor 2 is to account for the fact that only half the discharge goes to either side. Noting that

$$S_a = \sqrt{2}\ 0.38\ \frac{(g'_o q_o)^{1/3}(d-a)}{q_o} \qquad (13)$$

and substituting into equation (12) yields

$$a = \frac{4}{\pi}\ \frac{\sqrt{2}\ 0.38\ (g'_o q_o)^{1/3}(d-a)}{2}\ \ \frac{1+\frac{3}{2}C_D}{\frac{6}{\pi}g'_o q_o/2}$$

from which

$$\frac{a}{d} = \frac{\delta}{1+\delta}$$

where

$$\delta = \frac{2\sqrt{2}\ 0.38}{\pi}\left[\frac{1+\frac{3}{2}C_D}{\frac{3}{\pi}}\right]^{1/3} = \frac{2\sqrt{2}\ 0.38}{\pi}\left[\pi\left(\frac{1}{3}+\frac{C_D}{2}\right)\right]^{1/3} \qquad (14)$$

From experiments (see Figure 9), $C_D = 2.5$, hence $\delta = 0.40$ and

$$\frac{a}{d} = 0.29$$

In other words, the thickness of the sewage field should be 29% of the total depth. The depth of water available for mixing is d-a and is therefore 71% of the total depth. It is interesting to note that $0.71 \times \sqrt{2} \approx 1$ so that one may use the full depth d for y in equation (8) provided one interprets the result as average instead of centerline dilution.

(b) Shape of surface plume in a parallel current.

An overhead view of the spreading surface field from a long submerged diffuser might be as shown in figure 12 for the case where an ocean current of speed U flows parallel to the diffuser. Assuming that the fluid all travels at speed U, a Galilean transformation (moving with the current) indicates that $b(\frac{x}{U})$ should behave similar to b(t) in the solution presented previously. For x less than L, the length of the diffuser, the continuous injection case applies while for x larger than L, the instantaneous injection case applies. For the case interfacial shear is unimportant in the region $x < L$, b(x) should be proportional to x. For $x > L$, b(x) should be proportional to $x^{2/3}$. For very large x, (interfacial shear becomes important), b(x) should be proportional to $x^{1/5}$. Thus the horizontal extent of the surface field can be obtained by using this approximation in the case when a Galilean transformation is permitted. For low ocean current speed, the surface field would actually extend upstream and in that region, the approximation is no longer valid.

Summary and Conclusions

In this paper, the time dependent spreading of a buoyant fluid on the surface of a heavier fluid is investigated by casting the problem in the form of an initial value problem. By assuming that the shape of the spreading layer remains geometrical similar from one instant to the next, differential equations were derived for two-dimensional and axisymmetric configurations in both the instantaneous and continuous release cases. Laboratory experiments were compared with the analysis and the results were found to compare favorably. Similar analysis can also be performed for the submerged case of spreading in a density stratification.

The results of this analysis should prove of value in environmental fluid mechanics such as the spreading of wastewater or thermal effluent on the sea surface. A fundamental important finding from the analysis is that in the two-dimensional continuous release case, the thickness of the spreading layer would tend to infinity as time tends to infinity while in the axisymmetric case, the thickness tends to a constant. The extra dimension available for spreading in the three-dimensional case is apparently sufficient to prevent complete blocking of the flow (or inundation of the source). In an actual submerged discharge of wastewater from a long diffuser in an otherwise stagnant ambient, the thickness of the spreading layer could probably be represented by the value indicated by assuming $C_F = 0$ in the equation (5). This thickness is deduced to be 29% of the depth. The results of the analysis can also be applied to estimate the horizontal area covered by the surface field in the case of a parallel current.

Acknowledgment

The writer wishes to acknowledge the financial support of NSF (Grant ENG 75-02985) and EPA (Grant T900137-03-2). Thanks are also due Messrs. C. Almquist, P. J. W. Roberts, and J. C. Chen for permitting the use of some of their experimental data.

References

Almquist, C., "The Two-Dimensional Surface Spreading of a Buoyant Fluid into an Infinite Stagnant Environment," Student Lab Report for Env 112, Caltech, 1973.

Koh, R. C. Y. and Chang, Y. C., "Mathematical Model for Barged Ocean Disposal of Wastes," EPA-660/2-73-029, Dec. 1973.

Koh, R. C. Y. and Fan, L. N., "Prediction of the Radioactive Debris Distribution Subsequent to a Deep Underwater Nuclear Explosion," Tetra Tech Report TC129, 1968.

Koh, R. C. Y. and Fan, L. N., "Further Studies on the Prediction of the Radioactive Debris Distribution Subsequent to a Deep Underwater Nuclear Explosion," Tetra Tech Report TC-154, 1969.

Koh, R. C. Y. and Fan, L. N., "Mathematical Models for the Prediction of Temperature Distributions Resulting from the Discharge of Heated Water into Large Bodies of Water," EPA 16130 DWO 10/70, 1970.

Koh, R. C. Y. and Brooks, N. H., "Fluid Mechanics of Waste-Water Disposal in the Ocean," Ann. Rev. of Fluid Mech., Vol. 7, 1975.

Sharp, J. J., "Spread of Buoyant Jets at the Free Surface," J. Hyd. Div., Proc. ASCE, May 1969.

Sharp, J. J., "Unsteady Spread of Buoyant Surface Discharge," J. Hyd. Div., Proc. ASCE, Sept. 1971.